High-Performance Strain-Compensated InGaAs–GaAsP–GaAs ($\lambda = 1.17\ \mu$m) Quantum-Well Diode Lasers

Nelson Tansu, *Student Member, IEEE,* and Luke J. Mawst, *Senior Member, IEEE*

***Abstract*—This letter reports studies on highly strained and strain-compensated InGaAs quantum-well (QW) active diode lasers on GaAs substrates, fabricated by low-temperature (550 °C) metal–organic chemical vapor deposition (MOCVD) growth. Strain compensation of the (compressively strained) InGaAs QW is investigated by using either InGaP (tensile-strained) cladding layer or GaAsP (tensile-strained) barrier layers. High-performance $\lambda = 1.165\ \mu$m laser emission is achieved from InGaAs–GaAsP strain-compensated QW laser structures, with threshold current densities of 65 A/cm^2 for 1500-μm-cavity devices and transparency current densities of 50 A/cm^2. The use of GaAsP-barrier layers are also shown to significantly improve the internal quantum efficiency of the highly strained InGaAs-active laser structure. As a result, external differential quantum efficiencies of 56% are achieved for 500-μm-cavity length diode lasers.**

***Index Terms*—Diode lasers, epitaxial growth, InGaAs–GaAs quantum well, long-wavelength lasers, quantum-well lasers, semiconductor growth, semiconductor lasers, strain.**

I. Introduction

Long-wavelength (1.3 μm) active regions grown on GaAs substrates have potential for temperature-insensitive performance due to the larger bandgap discontinuities than found in conventional InP-based structures. Several approaches have been used to achieve long-wavelength emission on GaAs substrates, ranging from the use of In(Ga)As quantum dots (QDs) [1], InGaAs highly strained quantum wells (QWs) [2], and InGaAsN QWs [3].

Complexity in forming high-quality distributed Bragg reflectors (DBRs) on InP has caused the fabrication of long-wavelength ($\lambda = 1.3$ and $1.55\ \mu$m) InP-VCSELs to be challenging. The ease in forming high-quality AlGaAs-based DBRs on GaAs substrates, and the low-temperature sensitive active regions, makes long-wavelength ($\lambda = 1.3$ and $1.55\ \mu$m) VCSELs on GaAs substrates an attractive alternative [4]. Another potential application for long-wavelength VCSELs, with emission wavelengths 1.2-μm or longer, is to replace conventional 780–850-nm VCSELs for higher speed short-distance optical datalink application [5].

In this letter, we report studies on highly strained InGaAs–GaAs QW active region diode lasers, aimed to extend the emission wavelength toward 1.3 μm. We try to extend the emission wavelength using two mechanisms. The first mechanism is by growing the active regions at low temperature (550 °C). Previous studies have shown improvements in optical properties of low-temperature-grown highly strained epitaxial layers due to reduced dislocation density [6], [7]. The second mechanism is by implementing strain compensation to increase the effective critical thickness of the InGaAs QWs [7]. The use of strain compensation reduces the effective strain of the highly lattice mismatched InGaAs QW, allowing longer wavelength emission to be achieved [7]. Previous studies have also reported the use of tensile strain barriers of GaAsP surrounding InGaAs QWs are effective in improving the carrier confinement to the QW for 0.98-μm [8] and 1.06-μm [9] diode lasers. Improvement of the carrier confinement in the QW will result in low-temperature sensitivity for threshold current and differential quantum efficiency. The studies reported here indicate that the inclusion of GaAsP tensile barriers surrounding the highly strained (Δa/a $= 2.5\%$) InGaAs QW significantly improves the laser performance at $\lambda = 1.17\ \mu$m, resulting in low-threshold current densities (65 A/cm^2 for $L = 1500\ \mu$m) and higher internal quantum efficiencies compared with uncompensated structures.

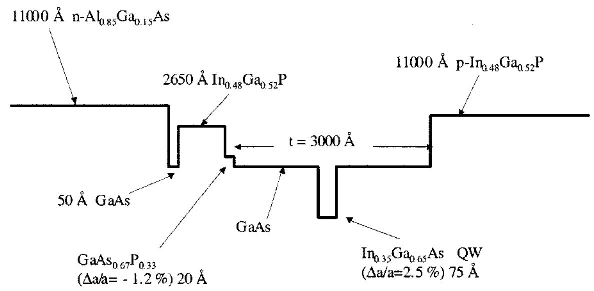

Fig. 1. Schematic energy bandgap diagram for the basic structure of the uncompensated 1.17-μm InGaAs QW edge-emitting lasers.

II. MOCVD Growth

All the laser structures studied here were grown by low-pressure (50 mbar) metalorganic chemical vapor deposition (LP-MOCVD). Trimethylgallium (TMGa), trimethylaluminum (TMAl), and trimethylindium (TMIn) are used as the group III sources, and AsH_3 and PH_3 are used as the group V sources. The dopants used here are SiH_4 and dielthylzinc (DEZn) for the n- and p-dopants, respectively.

The separate confinement heterostructure (SCH) containing a highly strained InGaAs QW-active region is shown schematically in Fig. 1. The n-cladding layer is composed of

Manuscript received September 7, 2000; revised December 1, 2000.

The authors are with the Reed Center for Photonics, Department of Electrical Computer Engineering, University of Wisconsin-Madison, Madison, WI 53706-1691 USA (e-mail: ntansu@students.wisc.edu).

Publisher Item Identifier S 1041-1135(01)01977-2.

n-$Al_{0.85}Ga_{0.15}As$ grown at a temperature of 800 °C. The use of n-AlGaAs for the lower cladding layer is to represent the DBRs for our future long-wavelength VCSEL structures. An additional u-$In_{0.48}Ga_{0.52}P$ cladding layer, grown at 700 °C, is used to enable us the possibility of incorporating the tensile-strained InGaP as a means of strain compensating the InGaAs active region. A thin u-GaAs transitional layer is grown between n-AlGaAs and the u-InGaP, so that the temperature ramping (800 °C–700 °C) is performed with GaAs on the top surface. The u-GaAs confining layers and InGaAs QW are both grown at 550 °C. We also employ a thin $GaAs_{0.67}P_{0.33}$ transitional layer [10] to improve the interface between the InGaP and GaAs layers, which is evident from the improved photoluminescence (PL) intensity and reduced PL full-width at half-maximum (FWHM) of the structures with the transitional layers of GaAsP.

The use of p-InGaP, grown at 650 °C, for the top cladding layer, is to enable us to avoid having to ramp up the temperature above 750 °C, which would be required for the growth of a high-quality p-AlGaAs cladding layer. In addition, the use of Al-free materials for the top cladding layer reduces series resistance, and simplifies the fabrication of regrown structures [12].

III. Device Structures and Photoluminescence Studies

All the diode laser structures studied here are similar to the basic structure shown schematically in Fig. 1, which has an optical field overlap (Γ) with the InGaAs QW of approximately 2.23%. The use of a single QW of 75-Å $In_{0.35}Ga_{0.65}As$ results in an emission lasing wavelength of approximately 1.16–1.17 μm. The peak wavelength of room temperature photoluminescence of all the structures is ranging from 1.150 to 1.158 μm.

The first structure (sample A) is the uncompensated structure, as shown in Fig. 1. This structure will be used for comparison purposes with strain-compensated structures. The FWHM of the room temperature PL is used to characterize the QW active region. For sample A, we measure a PL FWHM of 29 meV. In the second structure, sample B, we study is the use of a tensile-strained InGaP cladding layer as the mechanism to strain compensate the highly strained (2.5%) $In_{0.35}Ga_{0.65}As$ QW. The structure itself is similar to that of sample A, only the u-InGaP layer, grown prior to the GaAs confining region, is composed of 1900 Å of lattice-matched $In_{0.48}Ga_{0.52}P$ and 750 Å of tensile-strained ($\Delta a/a = -0.3\%$) $In_{0.44}Ga_{0.56}P$. The tensile-strained (−0.3%) $In_{0.44}Ga_{0.56}P$ is grown closest to the GaAs confining region. The FWHM of the PL for sample B is measured to be 26.5 meV, slightly reduced from sample A.

The third structure (sample C) uses tensile-strained GaAsP barriers to strain compensate the highly strained InGaAs QW, similar to that reported by Choi *et al.* [7] for different structures. The barriers are formed by 100-Å-thick tensile-strained ($\Delta a/a = -0.54\%$) $GaAs_{0.85}P_{0.15}$ layers on each side of the QW. Between the InGaAs QW and the tensile-strained barriers of GaAsP, 100-Å-thick GaAs transitional layers are used. Since the higher energy bandgap GaAsP layers closely surround the QW, they also enhance carrier confinement to the QW [9]. The FWHM of the PL for sample C is approximately 29 meV, slightly broadened compared to that of sample B.

TABLE I
Performance of InGaAs (Sample A), InGaAs–InGaP (Sample B), and InGaAs–GaAsP (Sample C) Diode Lasers for 100 μm-Wide × 1-mm-Long Devices. The Values in Parentheses Are the Values for Devices with Cavity Length of 1500 μm

	InGaAs	InGaAs/InGaP	InGaAs/GaAsP
λ(μm)	1.170	1.155	1.165
J_{th} (A/cm²)	150	135	70
J_{tr} (A/cm²)	100	89	50
η_d (%)	29	33	50
η_i (%)	37	38	61
α_i (cm⁻¹)	5	2	2
T_0 (K)	180 (450)	200 (450)	120 (180)
T_1 (K)	800 (600)	350 (400)	230 (300)

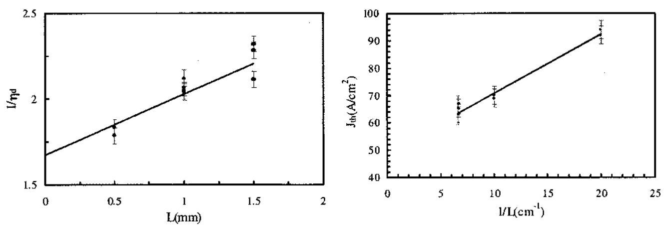

(a) (b)

Fig. 2. Threshold current density (a) and the external quantum differential quantum efficiency (b) of the InGaAs–GaAsP (sample C) as a function of cavity length.

IV. Laser Characteristics

The laser performance for the three different structures (samples A, B, C) are shown in Table I, as derived from length studies (see Fig. 2) on broad-area (100-μm wide) oxide-defined stripe lasers. From the table, we can see that a slight improvement had been achieved by using the tensile-strained InGaP cladding layer (sample B) to strain compensate the InGaAs QW. Greater improvement may be possible with this structure by reducing the separation between the InGaP and the InGaAs QW. Sample C is found to have the lowest threshold current density and highest efficiency of all three structures. However, the internal quantum efficiency from all three structures is much lower than values obtained from lower strained ($\lambda = 0.98$ μm) devices [8]. The low internal quantum efficiency is the primary reason that samples A and B have an external differential quantum efficiency ($L = 1000$ μm) of only 29% and 33%, respectively. The rather high values for the characteristic temperature coefficients for the threshold current density (T_0) and the differential quantum efficiency (T_1) for diode lasers form samples A and B are anomalous. These high values of characteristic temperature coefficients may be attributed to a high defect density in the QW. Carrier recombination through defects in the QW may be less temperature dependent, unlike the carrier leakage rates, which are highly temperature dependent. If nonradiative carrier recombination through defects significantly contributes to the threshold current, then the threshold current of the laser diode will be less sensitive to any temperature changes.

To investigate the cause of the low internal quantum efficiency, a structure similar to that shown in Fig. 1, was grown with a lower strain value ($\Delta a/a = 1.8\%$) for the QW, to ensure the critical thickness is not exceeded. This structure ex-

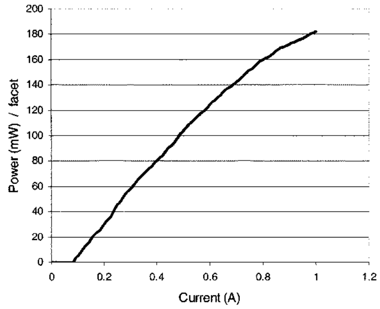

Fig. 3. Room temperature L–I curve under pulsed measurement with a pulsewidth of 6 μs, for the InGaAs–GaAsP (sample C) diode laser with cavity length of 1500 μm.

hibits similar values for internal quantum efficiency, indicating that the high strain is not responsible for low values obtained. However, the findings reported here are consistent with values reported by others [13] from similar active layer structures. Further studies are needed to investigate the low internal quantum efficiencies of these structures, although the low growth temperatures may be a factor.

The threshold and transparency current densities obtained from sample C are 70 A/cm^2 and 50 A/cm^2, respectively, which are quite low compared to other published data [5], [7] on similar structures. The inclusion of the GaAsP tensile barriers surrounding the QW may also improved the carrier capture in the QW, which is reflected in the improvement in the internal efficiency (61%). The highest differential quantum efficiency achieved for short cavity ($L = 500$ μm) is approximately 56%. The low duty-cycle (0.1%) pulsed output power versus current characteristics (P–I) are shown in Fig. 3. for a 500-μm-long device. The strong bending over of the P–I, as well as spectral measurements, indicates severe heating occurs as a result of a high device resistance [14]. Heating is less severe in long cavity devices ($L = 1.5$ mm), which have reasonably high values of T_0 (180 K). Similar bending in pulsed P–I curves has also been reported in previous publications [7]. The heating may be attributed to a highly resistive undoped GaAs confining region, presumably a result of the low temperature growth. A "*soft*" turn-on behavior was observed in the current versus voltage measurement of the devices. The differential series resistance of the devices is rather high (600 mΩ) compared to other published results (30 mΩ) [11]. These highly resistive GaAs confining regions could lead to low carrier capture efficiency, which results in a low internal quantum efficiency for the laser diode. The use of the GaAsP tensile-strained, high-energy bandgap barriers should increase the carrier capture, which will in turn lead to an increase the internal quantum efficiency.

V. Conclusion

We have demonstrated a very low threshold (65 A/cm^2, $L = 1500$ μm) and transparency current (50 A/cm^2) density diode lasers with an emission wavelength of 1.165 μm. The external differential quantum efficiency (56%, $L = 500$ μm) is limited by low internal quantum efficiency. The inclusion of the GaAsP tensile-strained barriers, surrounding the QW, has been shown to improve the internal efficiency, presumably due to an improvement in carrier capture efficiency. Optimization of GaAs confining regions to reduce the device resistance is needed. The optimal values of strain and thickness of the GaAsP tensile-strained barriers also needs further investigation. Finally, implementation of the N into strain-compensated InGaAs–GaAsP QW active region can be utilized to lead to high-performance long-wavelength (1.3-μm) semiconductor lasers.

Acknowledgment

The authors would like to acknowledge helpful technical discussions and assistances by Dr. M. R. T. Tan and Dr. S. W. Corzine at Agilent Technologies Laboratories.

References

[1] D. L. Huffaker, G. Park, Z. Zou, O. B. Shchekin, and D. G. Deppe, "1.3 μm room temperature GaAs-based quantum-dot laser," *Appl. Phys. Lett.*, vol. 73, pp. 2564–2566, 1998.
[2] F. Koyama, D. Schlenker, T. Miyamoto, Z. Chen, A. Matsutani, T. Sakaguchi, and K. Iga, "1.2 μm highly strained GaInAs/GaAs quantum well lasers for singlemode fiber datalink," *Electron. Lett.*, vol. 35, no. 13, pp. 1079–1081, 1999.
[3] S. Sato and S. Satoh, "Room-temperature continuous-wave operation of 1.24-μm GaInNA's lasers grown by metal-organic chemical vapor deposition," *IEEE J. Select. Topics Quantum Electron.*, vol. 5, pp. 707–710, May/June 1999.
[4] C. Wilmsen, H. Temkin, and L. A. Coldren, *Vertical-Cavity Surface-Emitting Lasers*. Cambridge, U. K.: Cambridge Univ. Press, 1999, ch. 8, p. 318.
[5] D. Schlenker, T. Miyamoto, Z. Chen, F. Koyama, and K. Iga, "1.17-μm highly strained GaInAs–GaAs quantum-well laser," *IEEE Photon. Technol. Lett.*, vol. 11, pp. 946–948, Aug. 1999.
[6] J. Y. Tsao, *Materials Fundamentals of Molecular Beam Epitaxy*. Boston, MA: Academic, 1993, ch. 5, pp. 183–186.
[7] W. Choi, P. D. Dapkus, and J. J. Jewell, "1.2-μm GaAsP/InGaAs strain compensated single-quantum well diode laser on GaAs using metal-organic chemical vapor deposition," *IEEE Photon. Technol. Lett.*, vol. 11, pp. 1572–1574, 1999.
[8] M. Sagawa, T. Toyonaka, K. Hiramoto, K. Shinoda, and K. Uomi, "High-power highly-reliable operation of 0.98-μm InGaAs–InGaP strain-compensated single-quantum-well lasers with tensile-strained InGaAsP barriers," *IEEE J. Select. Topics Quantum Electron.*, vol. 1, pp. 189–195, Mar./Apr. 1995.
[9] H. Asano, M. Wada, T. Fukunaga, and T. Hayakawa, "Temperature-insensitive operation of real index guided 1.06 μm InGaAs/GaAsP strain-compensated single-quantum-well laser diodes," *Appl. Phys. Lett.*, vol. 74, no. 21, pp. 3090–3092, 1999.
[10] Y. Kwon, W. G. Jeong, Y. Cho, and B. Choe, "Effect of $GaAs_yP_{1-y}$ $(0 < y < 1)$ interlayers on the structural, optical, and electrical characteristics of GaAs/InGaP heterojunction," *Appl. Phys. Lett.*, vol. 76, pp. 2379–2381, 2000.
[11] A. Al-Muhanna, L. J. Mawst, D. Botez, D. Z. Garbuzov, R. U. Martinelli, and J. Connolly, "14.3 W Quasicontinuous wave front-facet power from broad-waveguide Al-free 970 nm diode lasers," *Appl. Phys. Lett.*, vol. 71, no. 9, pp. 1142–1144, 1997.
[12] N. Tansu, D. Zhou, and L. J. Mawst, "Low-temperature sensitive, compressively strained InGaAsP active ($\lambda = 0.78 - 0.85$ μm) region diode lasers," *IEEE Photon. Technol. Lett.*, vol. 12, pp. 603–605, June 2000.
[13] Z. B. Chen, D. Schlenker, F. Koyama, T. Miyamoto, A. Matsutani, and K. Iga, "High temperature characteristics of highly strained 1.2-μm InGaAs/GaAs lasers," in *Proc. APCC/OECC'99*, vol. 2, Beijing, China, 1999, pp. 1311–1314.
[14] L. Shterengas, R. Menna, W. Trussell, D. Donetsky, G. Belenky, J. Connolly, and D. Garbuzov, "Effect of heterobarrier leakage on the performance of high power 1.5 μm InGaAsP multiple-quantum-well lasers," *J. Appl. Phys.*, vol. 88, no. 5, pp. 2211–2214, 2000.